

# Analysis of functionally graded carbon nanotubes reinforced composite panels using sublaminar variable-kinematics models

Alessio Gorgeri\*, Lorenzo Dozio†, Riccardo Vescovini‡

*Dipartimento di Scienze e Tecnologie Aerospaziali, Politecnico di Milano*

*Via La Masa 34, 20156 Milano, Italy*

## Abstract

---

The work regards the development of a numerical tool to study the mechanical response of multi-layered curved panels made of composite materials reinforced by carbon nanotubes with volume fraction graded along the thickness. The effective material properties of the composite material are estimated by means of the extended rule of mixture or the Eshelby-Mori-Tanaka method. The tool is based on sublaminar models with variable-kinematics description, therefore the applicability is not restricted to monolithic panels, on the contrary, the approach is well suited for sandwich panels with marked thickness-wise heterogeneity. Due to the efficiency of the formulation, the effect of various design parameters, either geometrical or mechanical, can be easily explored. The validation is performed against benchmarks of increasing complexities, namely a single-layer square plate, a shell reinforced by randomly oriented nanotubes, a sandwich panel with titanium alloy core and functionally graded skins. The importance of allowing kinematic descriptions of tunable accuracy within a unique framework is well demonstrated by the proposed assessments.

---

## 1. Introduction

Over the last few decades, the aerospace industry has witnessed the rapid advent of composite materials for load bearing and safety related parts. Exceptional mechanical properties such as high stiffness-to-weight and strength-to-weight ratios, fatigue and corrosion resistance, impact toughness are few of the many revolutionary aspects. On top of that, composite materials offer the chance to tailor the thermo-electro-mechanical properties of the structure by properly designing the reinforcement orientation, stacking sequence, material combination.

Newborn types of composites such as Functionally Graded Materials (FGM) further extend the design freedom by offering the chance to continuously vary such properties along the thickness direction of structural panels. The idea can be dated back to mid 1980s [1] with the development of a continuously graded metallic to ceramic heat barrier for hypersonic space-planes that could withstand extreme temperature gradients without failing to thermally induced interlaminar stresses.

The concept was then extended to panels reinforced with carbon nanotubes (serendipitously discovered by a Japanese scientist in 1991) to fabricate Functionally Graded Carbon Nanotubes Reinforced Composites (FG-CNTRC). The exceptional mechanical properties of nanotubes (average elastic modulus of about 1 TPa [2] and strength up to 63 GPa [3]) together with the aforementioned tailorability makes them the ideal candidate for next generation aerospace structures.

These exceptional characteristics however, are associated with an inherent complexity of the mechanical response that can be hardly predicted using conventional modelling strategies such as the Classical Lamination Theory (CLT). Rather

---

\*Former MSc student. Ph.D. candidate in Aerospace Engineering. *Email address:* alessio.gorgeri@polimi.it

†Associate Professor, Thesis advisor.

‡Assistant Professor, Thesis co-advisor.

than switching to inefficient 3D models, the common approach is to develop ad-hoc high-order kinematic formulations that are capable case-by-case to catch the peculiarities of the displacement field (non-linearities, piece-wise continuity, etc.), therefore tackle the problem with limited computational effort.

Here we go beyond the conventional frozen-kinematics theories thanks to a generalized approach that allows to build kinematic models of arbitrary complexity that can combine accuracy and efficiency in an optimal balance. The two pillars of the formulation are the concept of sublaminates and the variable-kinematics.

On the one hand, the idea of discretizing the thickness-domain in sublaminates comes from the observation that the most important variations of elastic properties are generally confined to a subset of layer interfaces – for instance, between the core and the facesheets in the case of a sandwich. Few examples of Zig-Zag enriched [4] and high order sublaminated models [5] are reported.

On the other hand, the idea of building a framework in which different kinematic theories could be systematically generated was from Carrera. The formulation – named after him as Carrera’s Unified Formulation or CUF – was then generalized by Demasi [6] to account for different orders of expansions of the displacements components. The formulation took the name of Generalized Unified Formulation or GUF.

The adoption of a variable-kinematics approach such as GUF in conjunction with a sublaminated description of the structure was first performed by D’Ottavio [7], who presented the so called Sublaminated-GUF (S-GUF).

Over the last few years, several solution techniques were explored within the S-GUF modelling framework. Here we adopt a Ritz approach, that has been successfully employed in the recent past for bending problems of composite laminated plates [8], thermo-mechanical problems, with particular regard to the thermal-buckling of sandwich plates [9], vibration of piezocomposite plates [10].

The Ritz-S-GUF modelling approach is here applied for the first time to functionally graded, multilayered cylindrical panels, as described in the following.

## 2. Mathematical formulation

A numerical formulation is here developed for cylindrical shells that can be applied to any structural configuration, in particular to multilayered panels with relevant thickness-wise variations of material properties (either piece-wise as for conventional sandwich panels or continuous as for FGM and FG-CNTRC), for which an optimal balance between accuracy and theory-related degrees of freedom can be obtained.

A sketch of a sandwich panel with laminated bottom skin and FG-CNTRC top skin is illustrated in Figure 1. Here we define the mid-surface curvature radius  $R$ , length  $a$ , arclength  $b = R\varphi$  and thickness  $h$ . The mid-surface is spanned by  $x \in [0, a]$  and  $y \in [0, b]$  while  $z \in [-h/2, h/2]$  spans the thickness-wise direction. The meaning of  $p$  and  $k$  is explained in the following section.

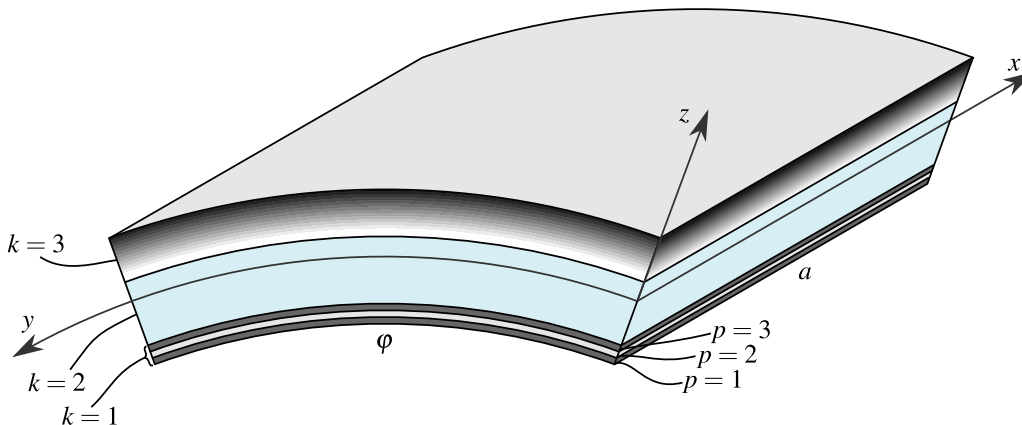


**Figure 1:** Sketch of a multi-layered shell structure. Highlighted is the ply-sublaminated description of S-GUF.

Both free-vibration and bending problems can be tackled. In the latter case, the shell is subjected to normal pressure acting on either internal or external surface

$$f_{\text{top}} = f_z^{\text{top}}(x, y, t) \quad f_{\text{bot}} = f_z^{\text{bot}}(x, y, t) \quad (1)$$

## 2.1. The Principle of Virtual Displacements

The equilibrium condition is expressed by means of the Principle of Virtual Displacements (PVD), which reads

$$\int_V \delta \boldsymbol{\varepsilon}^T \boldsymbol{\sigma} dV = - \int_V \delta \mathbf{u}^T \boldsymbol{\rho} \ddot{\mathbf{u}} dV + \int_{\Omega_{\text{top}}} \delta u_{\text{top}} f_{\text{top}} d\Omega_{\text{top}} + \int_{\Omega_{\text{bot}}} \delta u_{\text{bot}} f_{\text{bot}} d\Omega_{\text{bot}} \quad (2)$$

Here,  $\boldsymbol{\sigma}$  and  $\boldsymbol{\varepsilon}$  are the stress and strain vectors, respectively, the double-dot denotes second time derivative, and  $u_{\text{bot/top}} = u_z(x, y, \pm h/2)$  are the  $z$ -components of the displacement field evaluated at inner and outer surfaces  $\Omega_{\text{top}}$  and  $\Omega_{\text{bot}}$ , respectively. The elementary volume in the chosen reference frame is

$$dV = (1 + z/R) dx dy dz \quad (3)$$

where  $dx dy = d\Omega$  is the elementary mid-surface.

According to S-GUF, the panel is divided into a set of sublaminates, each comprising (one or more) adjacent plies with similar mechanical properties. Sublaminates are numbered from  $k = 1$  to  $k = N_k$  while plies are numbered locally within each sublaminate from  $p = 1$  to  $p = N_p^k$ . The formulation allows to build multiple-kinematics models (i.e. different theories are adopted in different thickness sub-regions simultaneously, effectively minimizing the number of overabundant degrees of freedom) within a variable-kinematics framework (i.e. a parametric approach that allows to build a virtually infinite number of kinematic theories in a simple and straightforward manner).

Once a proper kinematic model is postulated, the strain and stress components are obtained from the (unknown) kinematic variables of the model by means of gradient and constitutive laws. In the following, a generic quantity referred to the  $p$ -th ply of the  $k$ -th sublaminate is written as  $(\ )^{p,k}$ .

## 2.2. Constitutive equation for FG materials

Within the framework of linear elasticity, the Hooke's law for orthotropic materials reads

$$\boldsymbol{\sigma}^{p,k} = \tilde{\mathbf{C}}^{p,k} \boldsymbol{\varepsilon}^{p,k} \quad (4)$$

where  $\tilde{\mathbf{C}}^{p,k}$  if expressed in the structure reference frame and has the following non-null components

$$\tilde{\mathbf{C}}^{p,k} = \begin{bmatrix} \tilde{C}_{11}^{p,k} & \tilde{C}_{12}^{p,k} & \tilde{C}_{13}^{p,k} & 0 & 0 & \tilde{C}_{16}^{p,k} \\ \tilde{C}_{12}^{p,k} & \tilde{C}_{22}^{p,k} & \tilde{C}_{23}^{p,k} & 0 & 0 & \tilde{C}_{26}^{p,k} \\ \tilde{C}_{13}^{p,k} & \tilde{C}_{23}^{p,k} & \tilde{C}_{33}^{p,k} & 0 & 0 & \tilde{C}_{36}^{p,k} \\ 0 & 0 & 0 & \tilde{C}_{44}^{p,k} & \tilde{C}_{45}^{p,k} & 0 \\ 0 & 0 & 0 & \tilde{C}_{45}^{p,k} & \tilde{C}_{55}^{p,k} & 0 \\ \tilde{C}_{16}^{p,k} & \tilde{C}_{26}^{p,k} & \tilde{C}_{36}^{p,k} & 0 & 0 & \tilde{C}_{66}^{p,k} \end{bmatrix} \quad (5)$$

The effective elastic properties of each FG layer are obtained through an homogenization procedure, according to the rule of mixtures [11] or the Eshelby-Mori-Tanaka approach [12].

In the following we will assume a linear distribution of the reinforcement volume fraction within each ply, according to the following configurations that are technologically achievable in practice:

$$\begin{aligned} \text{UD} & : V_f(z) = V_f^* \\ \text{FG-V} & : V_f(z) = 2 \left( \frac{z}{h} + 0.5 \right) V_f^* \\ \text{FG-A} & : V_f(z) = 2 \left( -\frac{z}{h} + 0.5 \right) V_f^* \\ \text{FG-O} & : V_f(z) = 4 \left( \frac{|z|}{h} \right) V_f^* \\ \text{FG-X} & : V_f(z) = 4 \left( 0.5 + \frac{|z|}{h} \right) V_f^* \end{aligned} \quad (6)$$

where  $V_f(z)$  is the local CNTs volumetric fraction and  $V_f^*$  is the maximum volumetric fraction. The matrix volumetric fraction is simply

$$V_m(z) = 1 - V_f(z) \quad (7)$$

**2.2.1. Rule of mixture.** According to the rule of mixtures, the effective properties of the composite material are estimated by means of a weighted summation of stiffnesses or compliances, corrected with efficiency factors  $\eta_i$  which are introduced to match molecular-dynamics simulations, and can be written as

$$\begin{aligned} E_1 &= \eta_1 V_f E_1^f + V_m E_m \\ \frac{\eta_2}{E_2} &= \frac{V_f}{E_2^f} + \frac{V_m}{E_m} \\ \frac{\eta_3}{G_{12}} &= \frac{V_f}{G_{12}^f} + \frac{V_m}{G_m} \\ \nu_{12} &= V_f \nu_{12}^f + V_m \nu_m \end{aligned} \quad (8)$$

where  $E_1$  is the Young's modulus in the fibre direction,  $E_2$  is the Young's modulus in directions perpendicular to the fibres (therefore  $E_3 = E_2$ ),  $G_{12}$  is the shear modulus in a plane containing the fibre direction (therefore  $G_{13} = G_{12}$ ) and  $\nu_{12}$  is the Poisson's coefficient, ratio of the shrinkage in the 2-direction (normal to the fibre) and extension in 1-direction (fibre direction) when a load is applied in the fibre direction (therefore  $\nu_{13} = \nu_{12}$ ).

In addition, common assumptions for the other coefficients are either  $G_{23} = G_{12}$  ( $\nu_{23} = \nu_{12}$ ) or  $G_{23} = G_m$  ( $\nu_{23} = \nu_m$ ), and the matrix of elastic moduli  $\mathbf{C}$  is fully determined in the material frame.

**2.2.2. Eshelby-Mori-Tanaka.** The Eshelby-Mori-Tanaka method is an advanced approach based on micromechanics of inclusions/defects. The method is here applied to composites reinforced by straight, aligned CNTs and by randomly oriented straight CNTs. Additional application of the method include, but are not limited to, curved, partially or full agglomerated CNTs, of which examples can be found in [13].

**Straight, aligned CNTs** Let  $k, l, m, n,$  and  $p$  be the Hill's elastic moduli [14] of the composite material so that the constitutive relation is written in the material frame as

$$\begin{pmatrix} \sigma_x \\ \sigma_y \\ \sigma_z \\ \tau_{yz} \\ \tau_{xz} \\ \tau_{xy} \end{pmatrix}^{p,k} = \begin{bmatrix} n & l & l & 0 & 0 & 0 \\ l & k+m & k-m & 0 & 0 & 0 \\ l & k-m & k+m & 0 & 0 & 0 \\ 0 & 0 & 0 & m & 0 & 0 \\ 0 & 0 & 0 & 0 & p & 0 \\ 0 & 0 & 0 & 0 & 0 & p \end{bmatrix}^{p,k} \begin{pmatrix} \varepsilon_x \\ \varepsilon_y \\ \varepsilon_z \\ \gamma_{yz} \\ \gamma_{xz} \\ \gamma_{xy} \end{pmatrix}^{p,k} \quad (9)$$

where  $k$  is the plane-strain bulk modulus normal to the fiber direction,  $n$  is the uniaxial tension modulus in the fiber direction,  $l$  is the associated cross modulus,  $m$  and  $p$  are the shear moduli in planes normal and parallel to the fiber direction, respectively.

Let the mechanical behaviour of the matrix be described by  $E_m, \nu_m$  and  $\rho_m$ , and for the orthotropic CNTs by the Hill's moduli  $k_f, l_f, m_f, n_f, p_f$  and mass density  $\rho_f$ . According to the Eshelby-Mori-Tanaka theory, the Hill's moduli of the composite material are

$$k = \frac{E_m \left\{ E_m V_m + 2k_f (1 + \nu_m) [1 + V_f (1 - 2\nu_m)] \right\}}{2(1 + \nu_m) [E_m (1 + V_f - 2\nu_m) + 2V_m k_f (1 - \nu_m - 2\nu_m^2)]} \quad (10)$$

$$l = \frac{E_m \left\{ V_m \nu_m [E_m + 2k_f (1 + \nu_m)] + 2V_f l_f (1 - \nu_m^2) \right\}}{(1 + \nu_m) [2V_m k_f (1 - \nu_m - 2\nu_m^2) + E_m (1 + V_f - 2\nu_m)]} \quad (11)$$

$$\begin{aligned} n &= \frac{E_m^2 V_m (1 + V_f - V_m \nu_m) + 2V_m V_f (k_f n_f - l_f^2) (1 + \nu_m)^2 (1 - 2\nu_m)}{(1 + \nu_m) \left\{ 2V_m k_f (1 - \nu_m - 2\nu_m^2) + E_m (1 + V_f - 2\nu_m) \right\}} + \\ &+ \frac{E_m \left[ 2V_m^2 k_f (1 - \nu_m) + V_f n_f (1 - 2\nu_m + V_f) - 4V_m l_f \nu_m \right]}{2V_m k_f (1 - \nu_m - 2\nu_m^2) + E_m (1 + V_f - 2\nu_m)} \end{aligned} \quad (12)$$

$$p = \frac{E_m [E_m V_m + 2(1 + V_f) p_f (1 + \nu_m)]}{2(1 + \nu_m) [E_m (1 + V_f) + 2V_m p_f (1 + \nu_m)]} \quad (13)$$

$$m = \frac{E_m [E_m V_m + 2m_f(1 + v_m)(3 + V_f - 4v_m)]}{2(1 + v_m) \left\{ E_m [V_m + 4V_f(1 - v_m)] + 2V_m m_f(3 - v_m - 4v_m^2) \right\}} \quad (14)$$

and the elastic moduli matrix is recovered in the material frame.

**Randomly oriented CNTs** If the nanotubes are dispersed in the matrix without any prescribed orientation the resulting composite material is isotropic with elastic coefficients

$$E = \frac{9KG}{3K + G} \quad v = \frac{3K - 2G}{6K + 2G} \quad (15)$$

where  $K$  and  $G$  are the bulk and shear moduli that are computed as

$$K = K_m + \frac{V_f(\delta_f - 3K_m\alpha_f)}{3(V_m + V_f\alpha_f)} \quad G = G_m + \frac{V_f(\eta_f - 2G_m\beta_f)}{2(V_m + V_f\beta_f)} \quad (16)$$

where  $K_m$  and  $G_m$  are the bulk and shear moduli of the matrix and the other parameters are computed as

$$\alpha_f = \frac{3(K_m + G_m) + k_f - l_f}{3(G_m + k_f)} \quad (17)$$

$$\beta_f = \frac{1}{5} \left[ \frac{4G_m + 2k_f + l_f}{3(G_m + k_f)} + \frac{4G_m}{G_m + p_f} + \frac{2[G_m(3K_m + G_m) + G_m(3K_m + 7G_m)]}{G_m(3K_m + G_m) + m_f(3K_m + 7G_m)} \right] \quad (18)$$

$$\delta_f = \frac{1}{3} \left[ n_f + 2l_f + \frac{(2k_f + l_f)(3K_m + 2G_m - l_f)}{G_m + k_f} \right] \quad (19)$$

$$\eta_f = \frac{1}{5} \left[ \frac{2}{3}(n_f - l_f) + \frac{8G_m p_f}{G_m + p_f} + \frac{2(k_f - l_f)(2G_m + l_f)}{3(G_m + k_f)} + \frac{8m_f G_m(3K_m + 4G_m)}{3K_m(m_f + G_m) + G_m(7m_f + G_m)} \right] \quad (20)$$

where  $k_f$ ,  $l_f$ ,  $m_f$ ,  $n_f$ , and  $p_f$  are the Hills elastic moduli for the reinforcing phase.

The Hooke matrix is then built, whichever homogenization technique is used, to relate stresses and strains of the mean material.

The density of the composite material is always computed by the weighted summation of the constituents densities, which is

$$\rho = V_f \rho_f + V_m \rho_m \quad (21)$$

### 2.3. The gradient equations

Preserving the ply-sublaminar notation previously introduced, the strain-displacement relation for small deformations of cylindrical shells are

$$\varepsilon_x^{p,k} = \frac{\partial u_x^{p,k}}{\partial x} \quad (22)$$

$$\varepsilon_y^{p,k} = \frac{1}{1 + z/R} \left( \frac{\partial u_y^{p,k}}{\partial y} + \frac{u_z^{p,k}}{R} \right) \quad (23)$$

$$\gamma_{xy}^{p,k} = \frac{\partial u_y^{p,k}}{\partial x} + \frac{1}{1 + z/R} \frac{\partial u_x^{p,k}}{\partial y} \quad (24)$$

$$\gamma_{yz}^{p,k} = \frac{\partial u_y^{p,k}}{\partial z} + \frac{1}{1 + z/R} \left( \frac{\partial u_z^{p,k}}{\partial y} - \frac{u_y^{p,k}}{R} \right) \quad (25)$$

$$\gamma_{xz}^{p,k} = \frac{\partial u_x^{p,k}}{\partial z} + \frac{\partial u_z^{p,k}}{\partial x} \quad (26)$$

$$\varepsilon_z^{p,k} = \frac{\partial u_z^{p,k}}{\partial z} \quad (27)$$

where the flat plate equations are recovered setting  $1/R = 0$ .

## 2.4. The S-GUF and Ritz approximations

As previously mentioned, the unknown displacement components are expanded within each ply-sublaminates according to the chosen kinematic theory. The approximation is formally written as

$$\begin{cases} u_x^{p,k}(x, y, z_p, t) = F_{\alpha_{u_x}}(z_p) u_{x\alpha_{u_x}}^{p,k}(x, y, t) & \alpha_{u_x} = 0, 1, \dots, N_{u_x}^k \\ u_y^{p,k}(x, y, z_p, t) = F_{\alpha_{u_y}}(z_p) u_{y\alpha_{u_y}}^{p,k}(x, y, t) & \alpha_{u_y} = 0, 1, \dots, N_{u_y}^k \\ u_z^{p,k}(x, y, z_p, t) = F_{\alpha_{u_z}}(z_p) u_{z\alpha_{u_z}}^{p,k}(x, y, t) & \alpha_{u_z} = 0, 1, \dots, N_{u_z}^k \end{cases} \quad (28)$$

where  $F_{\alpha_{u_r}}$  are thickness functions and  $N_{u_r}^k$  is the order of expansion of the  $r$ -th displacement component within the sublaminates  $k$ . In the following,  $ED_{N_{u_x}, N_{u_y}, N_{u_z}}$  means an Equivalent Single Layer (ESL) theory, i.e. the plies of the  $k$ -th sublaminates share the same kinematic variables, while  $LD_{N_{u_x}, N_{u_y}, N_{u_z}}$  is a Layer-Wise (LW) theory of orders  $N_{u_x}, N_{u_y}, N_{u_z}$ .

The resulting 2D model is solved by means of a Ritz expansion of the kinematic variables, formally written as

$$\begin{cases} u_{x\alpha_{u_x}}^{p,k}(x, y, t) = N_{u_x j}(x, y) u_{x\alpha_{u_x j}}^{p,k}(t) \\ u_{y\alpha_{u_y}}^{p,k}(x, y, t) = N_{u_y j}(x, y) u_{y\alpha_{u_y j}}^{p,k}(t) \\ u_{z\alpha_{u_z}}^{p,k}(x, y, t) = N_{u_z j}(x, y) u_{z\alpha_{u_z j}}^{p,k}(t) \end{cases} \quad j = 1, 2, \dots, M \quad (29)$$

where  $N_{u_r j}$  are a complete set of boundary compliant shape functions.

The discrete form of the PVD is obtained after integrating the thickness and Ritz functions, either numerically or analytically when possible. The discretized PVD has the character of an indicial equation that has to be expanded over the theory-related and Ritz indexes, and assembled at ply-sublaminates levels to bring the problem to an easier-to-handle vector equation. The detailed steps can be found in [8], where the formulation was originally proposed for flat plates.

## 3. Results

A collection of comparisons against benchmarks of increasing complexities is here presented. Owing to the limited amount of literature dealing with multi-layer configurations, the potentialities of the formulation are somewhat partially exploited, though it is envisaged the tool be used in the near future for more complex problems.

### 3.1. Case study 1 – FG plate

The first example deals with bending and free vibrations of FG-CNTRC plates, for which numerical results were obtained by Zhu et al. [11]. The square plates ( $a/b = 1$ ) are fully clamped, have thickness  $h = 2$  mm and width-to-thickness ratios  $b/h = \{10, 20, 50\}$ .

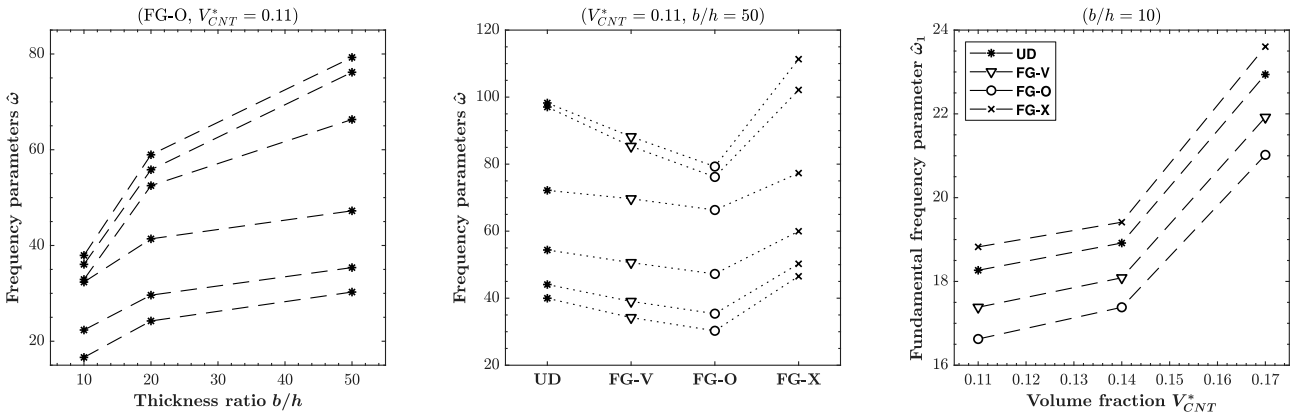


**Figure 2:** First six non-dimensional natural frequencies for several combinations of material and geometrical features.

The effective material properties of the two-phase nanocomposite, mixture of CNTs with  $E_1^c = 5.6466$  TPa,  $E_2^c = 7.0800$  TPa,  $G_{12}^c = 1.9446$  TPa,  $\nu_{12}^c = 0.175$ ,  $\rho^c = 1.4$  g/cm<sup>3</sup> and an isotropic polymer with  $E^m = 2.1$  GPa,  $\nu^m = 0.34$

$\rho^m = 1.15 \text{ g/cm}^3$ , are estimated through the rule of mixture of Eq. (8), with efficiency parameters being

$$\begin{aligned}
 \text{if } V_{\text{CNT}}^* = 0.11 &\rightarrow \eta_1 = 0.149, \eta_2 = 0.934 \\
 \text{if } V_{\text{CNT}}^* = 0.14 &\rightarrow \eta_1 = 0.150, \eta_2 = 0.941 \\
 \text{if } V_{\text{CNT}}^* = 0.17 &\rightarrow \eta_1 = 0.149, \eta_2 = 1.381
 \end{aligned} \tag{30}$$

in addition it is assumed that  $\eta_2 = \eta_3$ ,  $G_{23} = G_{13} = G_{12}$  and  $\nu_{23} = \nu_{13} = \nu_{12}$ .

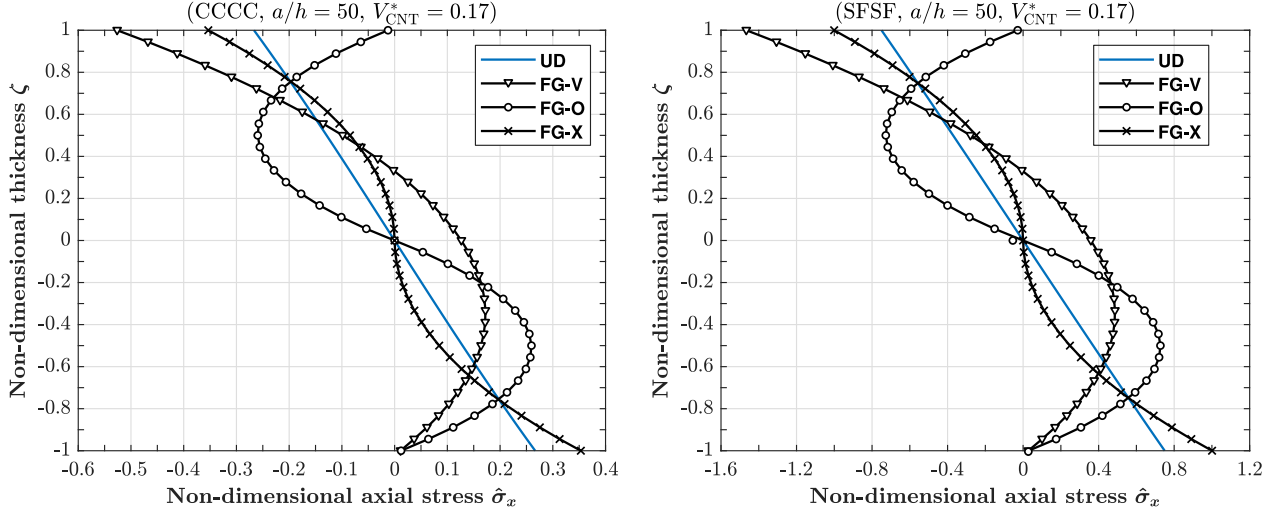


**Figure 3:** Non-dimensional axial stress evaluated through the thickness at  $x = a/2$ ,  $y = b/2$  for two kinds of support conditions and reinforcement distribution patterns.

The first 6 frequency parameters, defined as  $\hat{\omega}_i = \omega_i \frac{a^2}{h} \sqrt{\frac{\rho^m}{E^m}}$ , are computed by means of an high order theory (ED<sub>3,3,2</sub>) and 20 by 20 Ritz functions for several combinations of input parameters.

The obtained results are shown in Figure 2. It is clear from the middle and rightmost graphs that a relevant increase in natural frequency can be obtained by properly distributing the reinforcement phase. In particular, for the plate with  $b/h = 10$ , a difference of about 15% between FG-X (highest) and FG-O (lowest) fundamental frequencies is demonstrated, even at low reinforcement fraction. The trend is confirmed for all the frequency parameters that have been computed, regardless the combination of geometric parameters and reinforcement fraction.

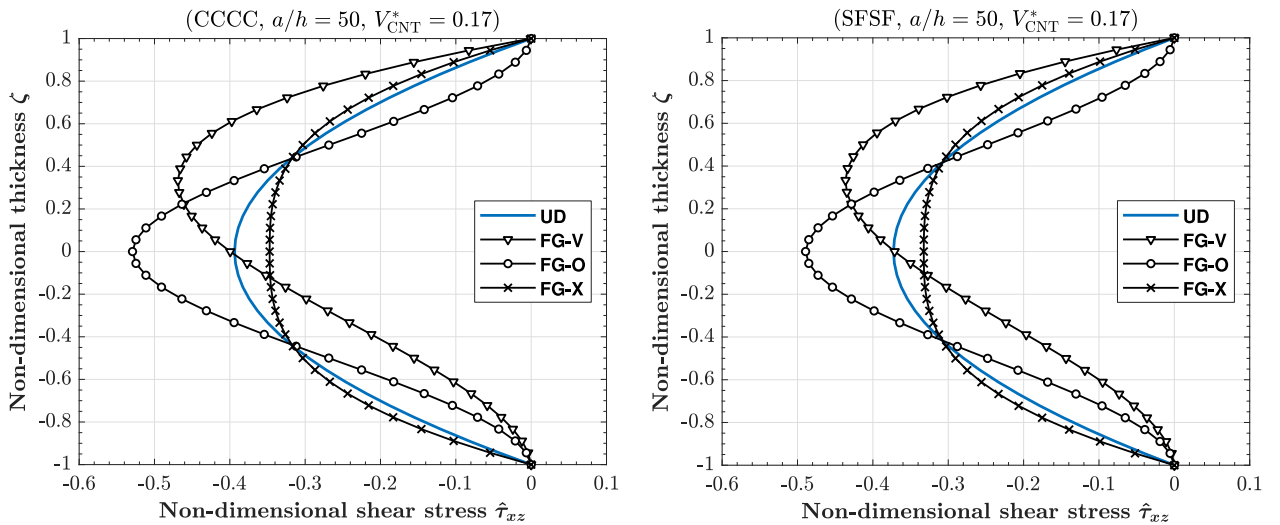


**Figure 4:** Non-dimensional transverse shear stress evaluated through the thickness at  $x = a/4$ ,  $y = b/2$  for two kinds of support conditions and reinforcement distribution patterns.

Bending results were also provided by the authors. Here we consider an uniformly distributed pressure  $f_0^{\text{top}} = -0.1$  MPa acting on the upper surface and two kinds of boundary conditions, CCCC and SFSF. The kinematic model is ED<sub>3,3,2</sub> with 25 by 25 Ritz functions.

The normalized axial stress  $\hat{\sigma}_x = \frac{h^2}{|f_0|a^2} \sigma_x$  evaluated through the thickness at  $x = a/2$ ,  $y = b/2$  and transverse shear stress  $\hat{\tau}_{xz} = \frac{h}{|f_0|a} \tau_{xz}$  evaluated through the thickness at  $x = a/4$ ,  $y = b/2$  and are shown in Figures 3 and 4, respectively, for width-to-thickness ratio  $b/h = 50$  and reinforcement volume fraction  $V_{\text{CNT}}^* = 0.17$ . Although similar patterns are observed for either the support conditions, the magnitudes are rather different. In general, a relevant through the thickness modulation of the stress components is demonstrated, for example: the maximum values of the in-plane normal stress of FG-O is located at about one quarter thickness rather than at the outer surfaces; the in-plane normal stress for FG-V is non-null at the mid-plane; the maximum transverse shear stress for the FG-X configuration is lower than UD.

### 3.2. Case study 2 – Shells reinforced with randomly oriented CNTs

A short excerpt of results dealing with curved panels is then presented, starting from a comparison with the ones delivered in [12]. The structure is a thick shell with radius-to-thickness ratio  $R/h = 10$ , angular width  $\varphi = \pi/4$ , length-to-radius ratio  $a/R = \{2, 5, 10\}$ . The straight edges are simply supported while the curved edges are either clamped-clamped or free-clamped. The chosen resin is PMMA with  $E_m = 2.5$  GPa and  $\nu_m = 0.34$  while the CNTs have  $E_1^c = 5.6466$  TPa,  $E_2^c = 7.0800$  TPa,  $G_{12}^c = 1.9446$  TPa,  $\nu_{12}^c = 0.175$ ,  $\rho^c = 1.4$  g/cm<sup>3</sup>. The nanotubes are randomly oriented and the mean properties of the resulting isotropic composite material are computed according to the Eshelby-Mori-Tanaka scheme. The kinematic model is ED<sub>5,5,4</sub> with 30 by 30 Ritz functions.

**Table 1:** Frequency parameter of the mode with one by one half-waves,  $\Omega_{1,1} = (R/\pi)^2 \sqrt{h\rho_m/D_m} \omega_{1,1}$ , for several combination of support, geometrical, material properties. Comparison with results delivered by Aragh.

BCs	$a/R$	UD		FG-V		FG-A		FG-O		FG-X	
		Aragh	Present	Aragh	Present	Aragh	Present	Aragh	Present	Aragh	Present
CSCS	2	N/A	12.9650	10.9280	10.9548	11.4262	11.4378	10.4184	9.9397	16.1171	15.2351
	5	N/A	10.2340	8.2904	8.3231	8.8180	8.8298	7.9288	7.3840	13.1674	12.3849
	10	N/A	9.9661	8.0390	8.0726	8.5711	8.5828	7.6971	7.1473	12.8637	12.0931
FSCS	2	N/A	10.2956	8.3574	8.3842	N/A	8.8789	N/A	7.4378	13.2169	12.4451
	5	N/A	9.9261	7.9497	8.0396	N/A	8.5474	N/A	7.1181	12.8101	12.0448
	10	N/A	9.8927	7.9719	8.0097	N/A	8.5186	N/A	7.0912	12.7723	12.0080

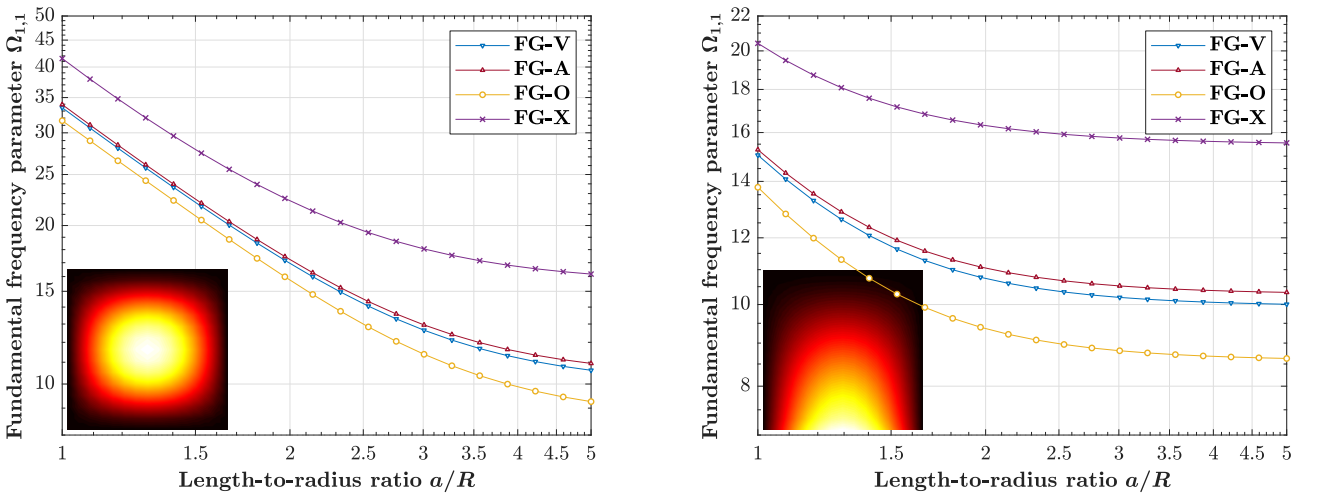


**Figure 5:** Fundamental frequency parameter vs length-to-radius ratio for a FG shell with  $R/h = 10$ ,  $\varphi = \pi/4$ . The inserts show the corresponding mode shape (the radial displacement is computed at the outer surface).

In Table 1 are collected the fundamental frequency parameters, defined as  $\Omega_{1,1} = (R/\pi)^2 \sqrt{h\rho_m/D_m} \omega_{1,1}$  with  $D_m =$

$E_m h^3 / (12(1 - \nu_m^2))$ , for all the possible combinations of geometric and material properties.

The same results are also displayed graphically in Figure 5 varying  $a/R$  for clamped-clamped (left) or clamped-free (right) curved edges and for several reinforcement deposition patterns. For low values of length-to-radius ratio we observe a linear decrement (in a logarithmic plot) of the fundamental frequency parameter. The curve becomes less steep as the ratio increases, eventually reaching a plateau. The frequency parameters becomes almost independent on the support conditions for  $a/R > 4$  because the curved edges becomes much shorter than the straight edges. A substantial improvement of the fundamental frequency can be ascribed to the FG-X configuration, for every combination of the other parameters.

### 3.3. Case study 3 – Sandwich plate with FG-CNTRC skins

The last example deals with bending of sandwich plates with functionally graded skins, for which results obtained by means of several kinematic theories were delivered in [15]. The authors recognized the need for adopting Zig-Zag enriched high-order models to catch the slope discontinuities at core-facesheets interfaces and the highly non-linear displacement field within FG plies.

**Table 2:** Displacement and stress components of a simply supported sandwich plate with FG skins loaded with bisinusoidally distributed pressure. Comparison of different ESL and LW theories. The proposed S-GUF model is  $ED_{3,3,2} / FSDT / ED_{3,3,2}$ .

Model DOFs	HSDT9	HSDT13	$ED_{1,1,0}$ 5	$ED_{3,3,2}$ 11	$ED_{6,6,5}$ 20	$LD_{1,1,0}$ 9	$LD_{3,3,2}$ 27	$LD_{4,4,3}$ 36	$LD_{5,5,4}$ 45	S-GUF 21
$\hat{u}_x$	0.6883	0.5463	0.9438	0.7325	0.7366	0.6047	0.6910	0.6911	0.6911	0.6921
$\hat{u}_z$	0.0847	0.1036	0.0760	0.0798	0.0799	0.1000	0.1023	0.1023	0.1023	0.1032
$\hat{\sigma}_x$	0.5747	0.4476	0.7084	0.5519	0.5554	0.4587	0.5242	0.5233	0.5235	0.5250
$\hat{\tau}_{xz}$	0.3926	0.4021	0.3794	0.3922	0.3872	0.3946	0.3928	0.3928	0.3930	0.3930
<b>Mean relative error:</b>			25%	8.4%	9.0%	6.9%	0.05%	0.01%	-	0.3%

0.54630.10360.44760.4021 0.68830.08470.57470.3926 The geometrical properties of the square ( $a/b = 1$ ) sandwich plate are: core-to-skin height ratio  $h_c/h_s = 2$  and length-to-height ratio  $a/h = 5$ . The stiff core is made by titanium alloy Ti-6Al-4V with  $E_c = 122.56$  GPa,  $\nu_c = 0.29$  and mass density  $\rho_c = 4.429$  g/cm<sup>3</sup>. The skins are made by Poly(methyl methacrylate) with  $E_m = 3.52$  GPa,  $\nu_m = 0.34$  and  $\rho_m = 1150$  kg/m<sup>3</sup>, reinforced by CNTs with  $E_1^c = 5.6466$  TPa,  $E_2^c = 7.0800$  TPa,  $G_{12}^c = 1.9446$  TPa,  $\nu_{12}^c = 0.175$ ,  $\rho^c = 1.4$  g/cm<sup>3</sup> with volume fraction graded along the thickness. The average reinforcement volume fraction and the corresponding efficiency parameters to be used in the extended rule of mixtures are  $V_{CNT}^* = 0.17$  with  $\eta_1 = 0.142$ ,  $\eta_2 = 1.626$ ,  $\eta_3 = 1.138$ , in addition it is assumed that  $G_{23} = 1.2G_{12}$  and  $\nu_{23} = \nu_{13} = \nu_{12}$ . The plate is fully simply supported and subjected to bi-sinusoidally distributed pressure load acting on the top surface  $f_z^{top}(x,y) = f_0 \sin(\pi x/a) \sin(\pi y/b)$  as shown in the insert of Figure 6. In the following, the normalized displacements and stress components are:

$$\hat{u}_x = 10 \frac{E_c}{hS^3 f_0} u_x(0, b/2) \quad \hat{u}_z = \frac{E_c}{hS^4 f_0} u_z(a/2, b/2) \quad \hat{\sigma}_x = -\frac{1}{S^2 f_0} \sigma_x(a/2, b/2) \quad \hat{\tau}_{xz} = \frac{1}{S f_0} \tau_{xz}(0, b/2) \quad (31)$$

where  $S = a/h$ .

A preliminary convergence assessment is performed, taking advantage of the ease to build several kinematic models offered by S-GUF. In Table 2 are collected results obtained by means of ESL and LW models of increasing complexity, compared with finite element models with 9 and 13 DOFs per element, from the referenced article. A sublaminar model, namely  $ED_{3,3,2} / FSDT / ED_{3,3,2}$  where FSDT stands for First Order Shear Deformation theory, is proposed as optimal trade-off between accuracy and number of DOFs (i.e. the number of kinematic variables, also shown in table).

It is inferred that high order ESL models are not suited for the problem in play, indeed, the abrupt change of material properties at core/skin interfaces produces a piece-wise continuous displacement field. For example, the mean relative error obtained with  $ED_{6,6,5}$  is higher than  $LD_{1,1,0}$ , despite employing twice the kinematic variables. Here the error is computed with respect to  $LD_{5,5,4}$  and averaged among displacements and stress quantities. It is observed that increasing the order of LW models beyond  $LD_{3,3,2}$  does not result in further accuracy improvements. The proposed S-GUF model further simplifies the kinematic description of the stiff core with respect to  $LD_{3,3,2}$ , without severe loss of accuracy.

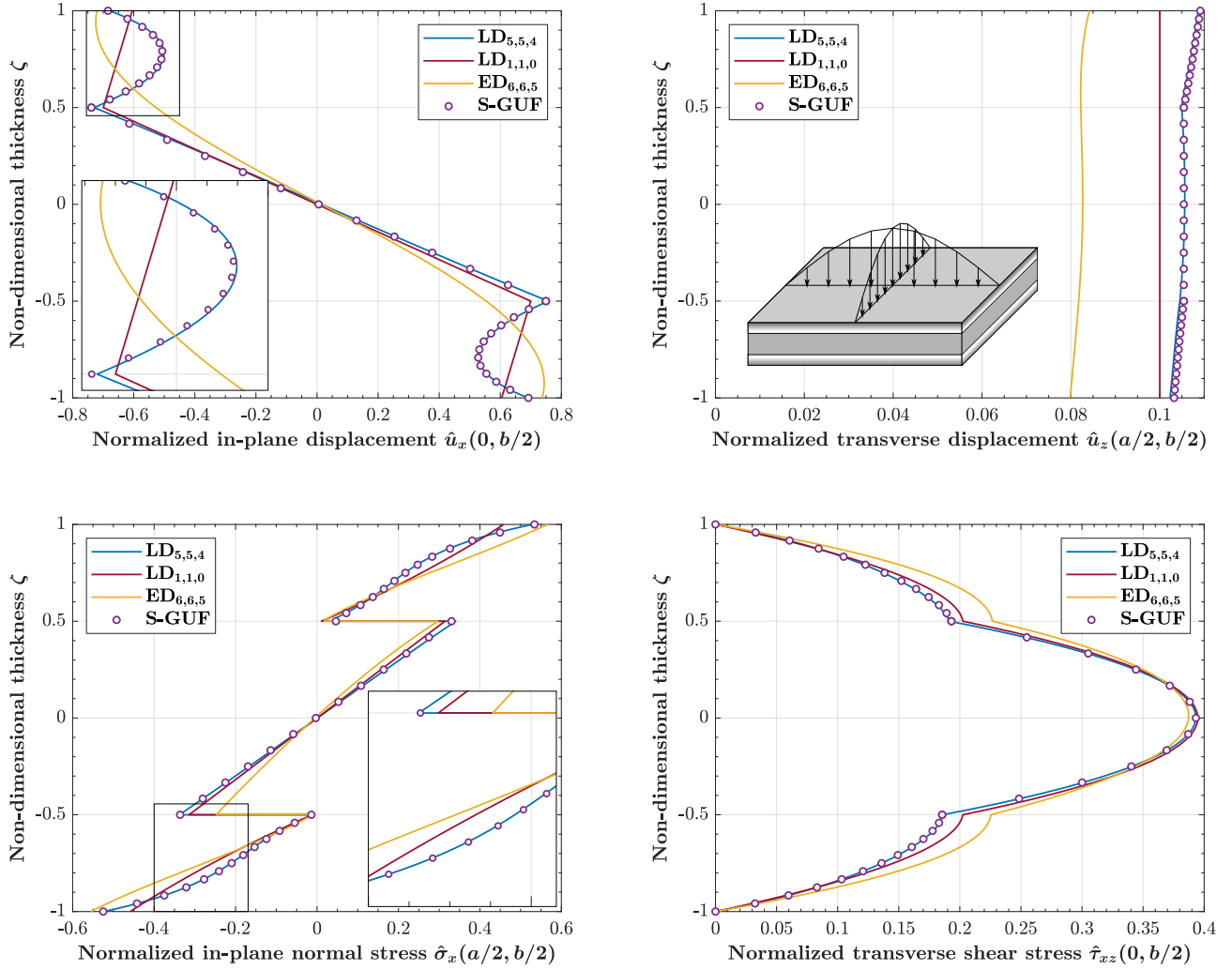


**Figure 6:** Normalized displacements and stress components for a sandwich panel with FG skins and  $a/h = 5$ ,  $h_c/h_s = 2$ ,  $V_{\text{CNT}}^* = 0.17$ . The plate is subjected to a bi-sinusoidally distributed pressure load acting on the upper surface  $f_z^{\text{top}}(x, y) = f_0 \sin\left(\frac{\pi x}{a}\right) \sin\left(\frac{\pi y}{b}\right)$ . Several kinematic models are proposed, where the S-GUF model is  $ED_{3,3,2}/\text{FSDT}/ED_{3,3,2}$ .

The through-the-thickness variations of displacement and stress components are shown in Figure 6. The graphs confirm that ESL models are completely unable to describe the displacement field, whilst the proposed S-GUF model allows to achieve quasi-3D accuracy by properly introducing a small set of kinematic variables.

The top-left graph demonstrate the importance of describing FG layers with high-order theories, in particular for FG-CNTRCs, where the continuous variation of mechanical properties and highly anisotropic behaviour typical of fibre reinforced plastic materials do coexist.

#### 4. Conclusions

The work has regarded the development and implementation of a tool for computing the free vibration and bending response of multilayered curved panels embedding functionally graded layers.

The shells are modelled within a variationally consistent generalized unified framework known as Sublaminated Generalized Unified Formulation (S-GUF), that makes it possible to obtain, within a single computer program, kinematic descriptions with adjustable accuracy and computational cost.

The goodness of the formulation is verified against benchmarks of increasing complexity, always demonstrating great prediction capabilities at very limited computational expense.

Benchmarks 1 and 2 are used to prove the validity of the formulation in dealing with monolithic structures. The

potentialities are then fully exploited in Benchmark 3 where a sandwich panel with functionally graded skins is concerned. The importance of allowing a multiple-kinematic description is highlighted by observing that the displacement field can be highly heterogeneous throughout the thickness, therefore hardly predictable with classical approaches. A small set of parametric analyses is also reported for Benchmarks 1 and 2, exploring the effect of material and geometrical features, while Benchmark 3 is mostly focused on a comparison of several kinematic models.

## References

- [1] M. Koizumi. FGM activities in Japan. *Composites Part B: Engineering*, 28(1):1 – 4, 1997.
- [2] J.P. Lu. Elastic properties of single and multilayered nanotubes. *Journal of Physics and Chemistry of Solids*, 58(11):1649 – 1652, 1997.
- [3] M.F. Yu, O. Lourie, M.J. Dyer, K. Moloni, T. Kelly, and R. Ruoff. Strength and breaking mechanism of multiwalled carbon nanotubes under tensile load. *Science*, 287(5453):637–640, 2000.
- [4] Y.B. Cho and R.C. Averill. First-order zig-zag sublaminar plate theory and finite element model for laminated composite and sandwich panels. *Composite Structures*, 50(1):1 – 15, 2000.
- [5] P. Frank Pai and A.N. Palazotto. Two-dimensional sublaminar theory for analysis of functionally graded plates. *Journal of Sound and Vibration*, 308(1):164 – 189, 2007.
- [6] L. Demasi.  $\infty^6$  Mixed plate theories based on the Generalized Unified Formulation. Part I: Governing equations. *Composite Structures*, 87(1):1 – 11, 2009.
- [7] M. D’Ottavio. A Sublaminar Generalized Unified Formulation for the analysis of composite structures. *Composite Structures*, 142:187 – 199, 2016.
- [8] M. D’Ottavio, L. Dozio, R. Vescovini, and O. Polit. Bending analysis of composite laminated and sandwich structures using sublaminar variable-kinematic Ritz models. *Composite Structures*, 155:45 – 62, 2016.
- [9] R. Vescovini, M. D’Ottavio, L. Dozio, and O. Polit. Thermal buckling response of laminated and sandwich plates using refined 2-D models. *Composite Structures*, 176:313 – 328, 2017.
- [10] M. D’Ottavio, L. Dozio, R. Vescovini, and O. Polit. The Ritz - Sublaminar Generalized Unified Formulation approach for piezoelectric composite plates. *International Journal of Smart and Nano Materials*, 9(1):34–55, 2018.
- [11] P. Zhu, Z.X. Lei, and K.M. Liew. Static and free vibration analyses of carbon nanotube-reinforced composite plates using finite element method with first order shear deformation plate theory. *Composite Structures*, 94(4):1450 – 1460, 2012.
- [12] B. Sobhani Aragh, A.H. Nasrollah Barati, and H. Hedayati. Eshelby-Mori-Tanaka approach for vibrational behavior of continuously graded carbon nanotube-reinforced cylindrical panels. *Composites Part B*, 43(4):1943–1954, 2012.
- [13] F. Tornabene, N. Fantuzzi, M. Baccocchi, and E. Viola. Effect of agglomeration on the natural frequencies of functionally graded carbon nanotube-reinforced laminated composite doubly-curved shells. *Composites Part B: Engineering*, 89:187 – 218, 2016.
- [14] R. Hill. A self-consistent mechanics of composite materials. *Journal of the Mechanics and Physics of Solids*, 13(4):213 – 222, 1965.
- [15] S. Natarajan, M. Haboussi, and M. Ganapathi. Application of higher-order structural theory to bending and free vibration analysis of sandwich plates with CNT reinforced composite facesheets. *Composite Structures*, 113:197–207, 2014.